Int J Thermophys (2011) 32:1697–1706
DOI 10.1007/s10765-011-1031-x

Monochromator-Based Absolute Calibration of Radiation Thermometers

T. Keawprasert · K. Anhalt · D. R. Taubert · J. Hartmann

Received: 30 March 2010 / Accepted: 23 June 2011 / Published online: 7 August 2011

Abstract A monochromator integrating-sphere-based spectral comparator facility has been developed to calibrate standard radiation thermometers in terms of the absolute spectral radiance responsivity, traceable to the PTB cryogenic radiometer. The absolute responsivity calibration has been improved using a 75 W xenon lamp with a reflective mirror and imaging optics to a relative standard uncertainty at the peak wavelength of approximately 0.17 % ($k = 1$). Via a relative measurement of the out-of-band responsivity, the spectral responsivity of radiation thermometers can be fully characterized. To verify the calibration accuracy, the absolutely calibrated radiation thermometer is used to measure Au and Cu freezing-point temperatures and then to compare the obtained results with the values obtained by absolute methods, resulting in $T - T_{90}$ values of +52 mK and −50 mK for the gold and copper fixed points, respectively.

Keywords Radiation thermometer · Spectral responsivity · Thermodynamic temperature measurement · $T - T_{90}$

Asterisks in the text represent references to commercial products and are provided for identification purposes only and constitute neither endorsement nor representation that the item identified is the best available for the stated purpose.

T. Keawprasert (✉) · K. Anhalt · D. R. Taubert · J. Hartmann
Physikalisch-Technische Bundesanstalt Braunschweig und Berlin,
Abbestrasse 2-12, 10587 Berlin, Germany
e-mail: thada.keawprasert@ptb.de

T. Keawprasert
National Institute of Metrology (Thailand), 3/4-5 Moo 3, Klong 5, Klong Luang,
12120 Pathumthani, Thailand

1 Introduction

Filter radiometers with interference filters are regularly used at PTB to measure thermodynamic temperatures in the irradiance mode [1]. Recently, these filter radiometers have been applied to measure indirectly the thermodynamic temperature of small aperture high-temperature fixed points with uncertainties comparable to those achievable with methods according to ITS-90 [2]. However, direct measurements of the thermodynamic temperature of these fixed points with small apertures require imaging systems. For these imaging systems the spectral radiance responsivity must be absolutely known.

Experimental setups with tunable or fixed-wavelength lasers as radiation sources for spectral responsivity calibrations have been reported in the literature [3–7]. For a calibration in the radiance mode, the laser output is coupled into an integrating sphere to generate a uniform Lambertian radiance. The laser-based method requires a series of tuneable lasers to measure the absolute responsivity in the required wavelength range directly or a laser providing single wavelengths around the center wavelength of the radiation thermometer in combination with the relative spectral responsivity measured with a monochromator-based method. However, interference fringes of up to several percent have been observed especially in the band-pass region of the radiation thermometer using laser-based systems [8,9]. In this case, measurements with small wavelength steps of around 10 pm are required to accurately follow the interference structure. Such measurements are extremely time consuming and not possible in every case; thus, an incomplete averaging may introduce significant errors.

Recently, a monochromator-based integrating sphere facility has been developed at PTB to provide monochromatic Lambertian radiation in the spectral range between 400 nm to 1100 nm [10]. One advantage of this setup is that an optimal spectral bandwidth can be selected in order to avoid any interference fringes in the spectral radiance responsivity. However, the dynamic range of the facility is lower than that of a PTB laser-based facility by more than two orders of magnitude when using a QTH lamp as a radiation source. The relative combined standard uncertainty is limited to 0.25 % ($k = 1$) by the maximum power of such a radiation source and the resulting signal-to-noise ratio of the radiation thermometer under test. Since the uncertainty due to noise decreases with increasing radiant power, the standard uncertainty of the calibration at the monochromator-based facility can be, in principle, reduced by increasing the input radiant power of the monochromator.

The ultimate goal of the present study is to improve the accuracy of the monochromator-based absolute calibration of radiation thermometers. A description of the facility and the calibration results of a radiation thermometer are presented. In order to verify the calibration accuracy, the absolute calibrated radiation thermometer is used to measure the Au and Cu freezing-point temperatures and the resulting $T - T_{90}$ values at these temperatures are presented.

2 Experimental Setup

A schematic diagram of the monochromator-based facility is shown in Fig. 1. The system consists of an XBO 75 W Xe-arc lamp from OSRAM* with a reflective mirror and

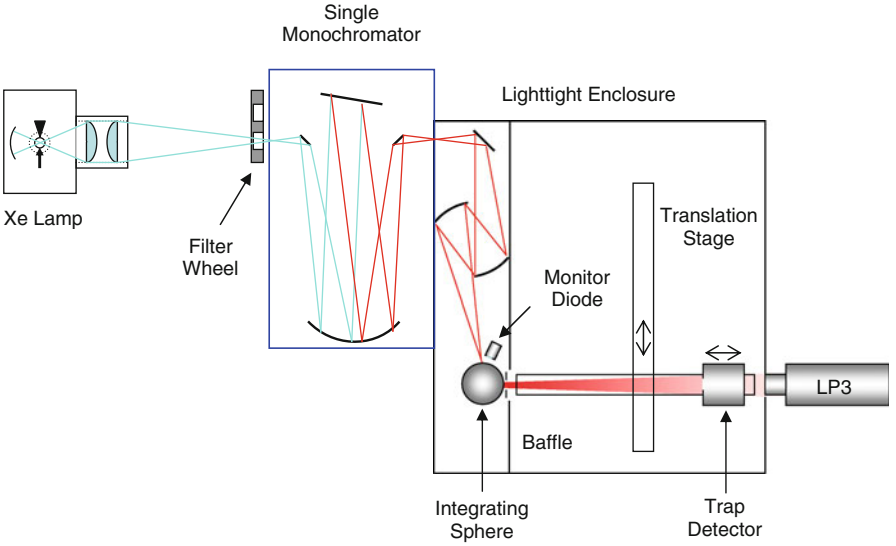

Fig. 1 Schematic diagram of the monochromator-based calibration facility

condensing lens unit, a single monochromator, and an integrating sphere. The superposed radiation, composed of the direct radiation and the reflected radiation from the xenon-arc lamp radiating with an f-number of 3, is imaged onto the entrance slit of the monochromator (SPM2, Zeiss)* with an f-number of 10 to match the optical geometry of the monochromator by using a pair of achromatic lenses. Since the Xe-arc lamp also produces intensive UV radiation, a filter wheel with appropriated band-pass filters has to be used, for instance, a filter WG 360 for the wavelength range of 370 nm to 720 nm. To enable a higher throughput, a single monochromator is used instead of a double monochromator. The wavelength selection of the radiation is performed using a precision diffraction grating with 1300 lines/mm (reciprocal dispersion of 2 nm/mm), whereas the wavelength calibration is performed at 50 spectral lines of different spectral lamps in the wavelength from 370 nm to 1100 nm with a standard uncertainty of 26 pm ($k = 1$) in the visible region. Since a bandwidth of at most 1 nm is required for the calibration of narrow band radiation thermometers, the entrance and exit slit widths of the monochromator are set to 0.5 mm. With such slit widths, the optical power at the exit slit ranges from 0.1 $\mu W \cdot nm^{-1}$ at 400 nm to more than 1 $\mu W \cdot nm^{-1}$ from 500 nm to 700 nm.

In contrast to measurements in the irradiance mode, for radiance mode measurements the radiation behind the exit slit is focused onto an entrance port of an integrating sphere with a diameter of 5.1 cm (2 in) by using a mirror system. A precision copper aperture of a nominal diameter of 5 mm is used to define the radiating area for calculating the spectral radiance by absolute measurements. For relative spectral responsivity measurements, the integrating sphere is replaced by a mirror and an adjustable aperture to feed the spectral radiation with a matching f-number into the optical setup of the radiation thermometer. To minimize the effect of diffuse stray light radiation, a blacken variable diameter aperture is placed between the integrating sphere and the

detectors. A monitor diode is also installed to correct for short-term variations during the measurements. Measurements were performed by direct substitution at each selected wavelength by using a translation stage to move the trap detector relative to a fixed position at a certain distance in front of the radiation thermometer in a light-tight box.

At this facility, radiation thermometers were calibrated in terms of their spectral radiance responsivity by comparison to an absolutely calibrated three-element Si trap detector, traceable to the primary cryogenic radiometer of PTB in terms of spectral power responsivity at several wavelengths [11]. In combination with two diamond-turned precision apertures, the trap detector can be employed to calculate the absolute spectral radiance by measuring the spectral irradiance. With known effective areas of the apertures and the distance between these two apertures, the geometric factor of the radiance measurement can be calculated. The aperture areas have been separately calibrated with the method described in [11] based of a laser scanning microscope method. As perfect knife edges are obtained, the effective area is independent of the angular distribution of the incoming radiation. The distance between these two apertures is accurately determined by a precision length gauge and an interferometer. With the absolute spectral power responsivity of the trap detector and the geometric factor of the measurement, the absolute spectral radiance can be calculated via the measured spectral irradiance [11]. The calculated spectral radiance is then compared to the photocurrent generated by the radiation thermometer to determine the absolute spectral radiance responsivity of the radiation thermometer via

$$S_{\mathrm{RT}}^{L}(\lambda) = G\,\frac{I_{\mathrm{ph,RT}}}{I_{\mathrm{ph,Trap}}}\,S_{\mathrm{Trap}}^{E}(\lambda), \tag{1}$$

where G is the geometric factor, $I_{\mathrm{ph,RT}}$ and $I_{\mathrm{ph,Trap}}$ are the photocurrents obtained from the radiation thermometer and the trap detector, respectively, and $S_{\mathrm{Trap}}^{E}(\lambda)$ is the spectral irradiance responsivity of the trap detector.

3 Uncertainty Estimation

Relevant uncertainty components for the absolute spectral radiance calibration of the monochromator-based setup are given in Table 1. All components are given as standard uncertainties at a coverage factor of $k = 1$. One of the main contributions is the spatial uniformity of the spectral radiance across the integrating sphere opening, which is expected to decrease for an increasing sphere diameter. However, a larger integrating sphere is not a straightforward solution to solve this problem, because for a fixed opening area, the output radiance quadratically decreases with an increasing sphere radius. Presently, the best radiance uniformity across the 5 mm aperture for the 5.1 cm (2 in) integrating spheres at the monochromator-based facility is ± 0.2 %, measured by scanning the aperture with the radiation thermometer under test at 650 nm with a bandwidth of 9 nm as shown in Fig. 2. Although a correction of the non-uniformity can be applied for any measurement, it increases the overall uncertainty due to the uncertainty of the uniformity measurement.

Table 1 Summary of the relative standard uncertainty contributions of the absolute spectral responsivity of the LP3 8005

Contributions of uncertainty	Monochromator-based (%) ($k = 1$)
Source instability	0.067
Spatial homogeneity	0.115
Spectral responsivity trap	0.025
Aperture area	0.013
Distance	0.050
Diffraction at two apertures	0.051
LP3 stability and noise	0.053
Effective wavelength	0.046
Squared sum	0.169

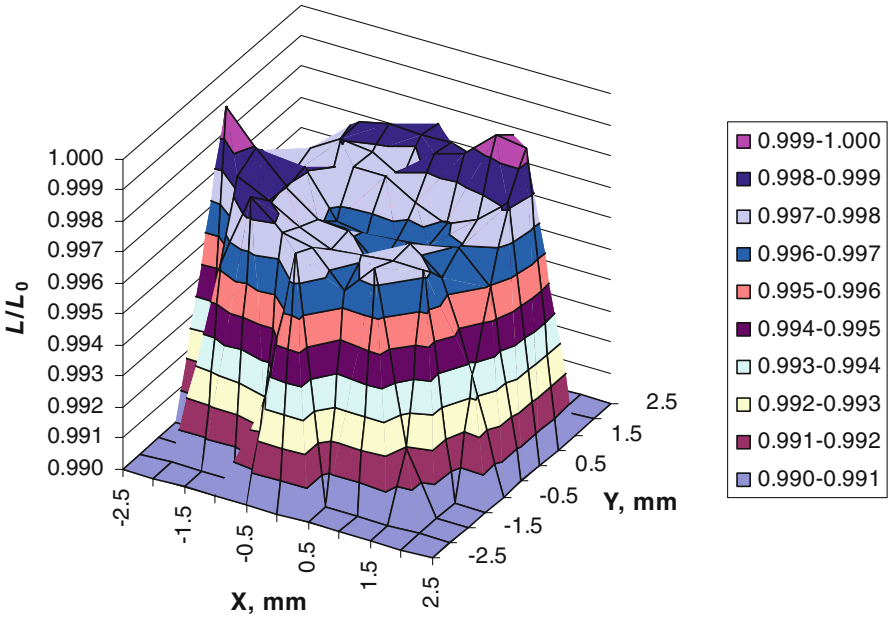

Fig. 2 Measured spatial uniformity of the spectral radiance across the radiating opening of the integrating sphere at 650 nm with a bandwidth of 9 nm

Since the uncertainty attributed to noise decreases with increasing radiant power, the repeatability of the integral responsivity is currently improved to better than 1×10^{-3} for the monochromator-based method due to the higher radiance of the Xe lamp in comparison to the QTH lamp. Although a correction due to the temporal instability of the radiation sources was applied by using the monitor diode, the uncertainty due to the temporal instability for the time interval of about 2 min is still 0.07 % due to the rapid fluctuations of the radiation emitted by the Xe lamp.

An uncertainty in the wavelength of less than 26 pm is obtained due to the temperature-controlled room and the careful wavelength initialization by using a mercury spectral lamp prior to every measurement. Finally, the overall uncertainty at the setup is within 0.17 % ($k = 1$). At this stage, a correction due to nonlinearity of the radiation thermometer under test was not considered, even though both of the absolute calibrations are performed at different signal levels, because recent results showed no significant non-linearity of the used radiation thermometer [12].

4 Calibration Results

4.1 Absolute Spectral Responsivity

In this article, the spectral radiance responsivity of a radiation thermometer LP3 (Ser. No. 80-05)* equipped with a 650 nm interference filter was absolutely calibrated for application to high-temperature measurements. At first a series of relative measurements without the integrating sphere was performed to investigate the performance of the single monochromator and to characterize the fine structure of the LP3's interference effect with different bandwidths. In the wavelength range from 400 nm to 1000 nm, measurements were conducted with bandwidths of 1 nm and 5 nm to measure the stray light of the monochromator. It was found that the stray-light level for this single monochromator is suppressed to less than 10^{-5} even for a monochromator bandwidth of 1 nm. As a result, the out-of-band responsivity of the LP3 on this setup will be limited by this level.

Within the band-pass region of the LP3's interference filter, relative measurements were performed with spectral bandwidths of 0.2 nm and 0.1 nm to find the optimum spectral bandwidth for calibration of the radiation thermometer. An oscillation pattern was not observed even for a bandwidth of 0.1 nm, which is in contrast to previous results obtained with another LP3 (Ser. No. 8013) as shown in Fig. 3 [10]. However, since the relative difference between the integral responsivity for 0.2 nm and 0.1 nm is less than 5×10^{-4}, a spectral bandwidth of 0.2 nm is used in favor of a time effective measurement.

By applying an integrating sphere for absolute calibration, the dynamic range of the monochromator setup was lower than that for the relative measurement, whereas most of the total radiation was directly introduced onto the LP3's field of view. With an effective bandwidth of 1.0 nm, the signal-to-noise ratio of the LP3 at the peak wavelength was approximately 10^3, using an integrating sphere of 5.1 cm (2 in) in diameter for a signal averaging time of 5 s. With the expected bandwidth of 0.2 nm, the LP3's signal-to-noise ratios were lower than the required level ($\geq 10^3$); hence, a spectral bandwidth of 1 nm is applied to measure in the band-pass region (650 nm $\pm$ 15 nm) for the absolute measurement. During the calibration, five runs were taken to evaluate the repeatability of the measurements, resulting in a relative repeatability of the integral responsivity of 5.3×10^{-4}. The repeatability of the effective wavelength for each run is better than 25 pm. In the blocking region, the results of the relative measurements were used by adjusting them with an absolute result at the peak wavelength to determine the absolute out-of-band responsivity of the LP3.

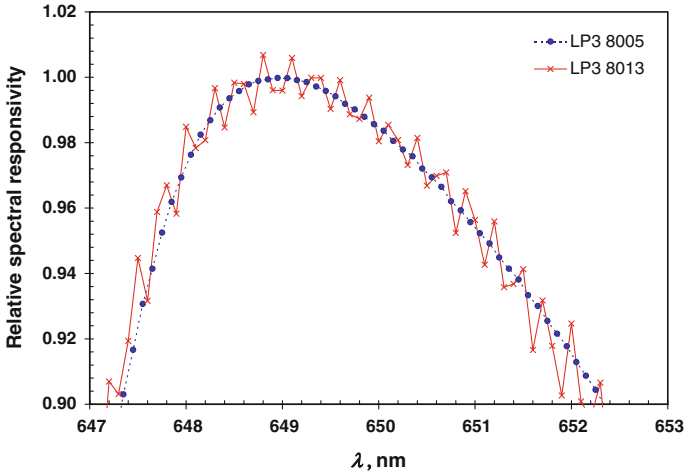

Fig. 3 Relative spectral radiance responsivity of the LP3.8005 and LP3 8013 with the spectral bandwidth of 0.1 nm measured at the monochromator-based setup

The absolute spectral radiance responsivity of the LP3 is plotted over the measurement range on a logarithmic scale in Fig. 4a and on a linear scale in Fig. 4b, in combination with the relative results with a bandwidth of 0.2 nm. It can clearly be seen that out-of-band suppression of the LP3 by the monochromator-based measurement for the relative measurement is less than 10^{-5} in the wavelength range from 400 nm to 1000 nm.

4.2 Measurement at the Au and Cu Fixed Points

To check the accuracy of the absolute calibration, the LP3 under test was applied to measure the photocurrents at ITS-90 fixed points, such as gold and copper, and compare these with photocurrents calculated based on the calibrated spectral responsivity. The calculated photocurrents at any thermodynamic temperature of a blackbody can directly be determined from integration of the absolutely calibrated radiance responsivity multiplied by Planck's function according to

$$i_{\mathrm{ph}} = \int S^{L}_{\mathrm{RT}} L(\lambda, T)\mathrm{d}\lambda, \tag{2}$$

where i_{ph} is the calculated photocurrent, S^{L}_{RT} is the absolute spectral radiance responsivity of the radiation thermometer, and $L(\lambda, T)$ is the spectral radiance given by Planck's law at the temperature of the gold or copper fixed-point temperature. The calculated photocurrents at the fixed-point temperatures assigned by ITS-90 should be in agreement with the measured values within their combined uncertainties.

In this measurement, an established gold fixed-point blackbody of PTB was used. All performances and details of this blackbody on differences in plateau shape and repeatability can be found in [13]. The emissivity of the cavity has been calculated

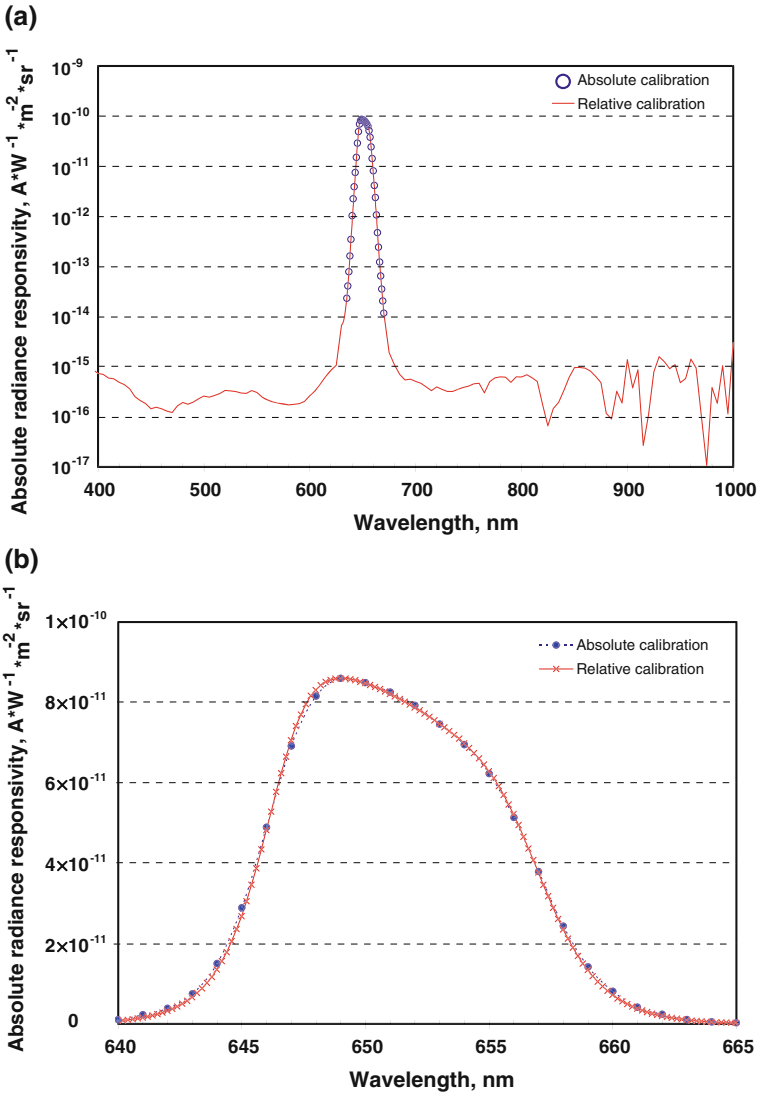

Fig. 4 Absolute spectral radiance responsivity of the LP3 8005 measured on the monochromator-based facility: (a) on a logarithmic scale, and (b) close to fine structure on a linear scale

to be 0.999988. For Cu, a small fixed-point cell manufactured by PTB [14] was employed by operating it inside a Nagano M furnace*. The emissivity of the Cu fixed-point cell is calculated to be 0.9997 (±0.0003) using a Monte Carlo technique based on the geometry of the crucible cavity [11]. The effective emissivities were considered to correct the measured signals.

To observe the photocurrents at the fixed points, the calibrated LP3 was aligned to the center of the cavity opening of the fixed-point cells at a distance of 700 mm. Melts and freezes were performed by varying the furnace temperature in steps of ±5 K for

Table 2 Summary of the measured and calculated photocurrents of the LP3 8005 at the fixed-point temperatures using the calibrated absolute spectral responsivity

Fixed point	Measured photocurrent (A)	Calculated photocurrent (A)	Relative difference (%)	Combined uncertainty $k = 1$ (%)	Thermodynamic temperature (K)
Au	6.431×10^{-11}	6.427×10^{-11}	−0.07	0.19	1064.232 ± 0.154
Cu	8.235×10^{-11}	8.240×10^{-11}	0.06	0.20	1084.570 ± 0.158

the Au fixed point and ±25 K for the Cu point, with respect to the temperature defined by ITS-90. During the freezing plateau of the fixed points, the signal is stable within the relative standard deviation of 1.2×10^{-4} over a period of more than 5 min for the copper blackbody and 1 h for the gold blackbody. The photocurrents at the freezing temperatures can be estimated as the average between 25 % and 75 % solid fractions of the freeze plateau. For each fixed point, a difference between this average value and the maximum of the freezing curve is less than 2.4×10^{-4}.

A summary of the corrected photocurrents at the Au and Cu freezing temperatures measured by the LP3 under test is shown in Table 2, along with the calculated photocurrents and the obtained thermodynamic temperatures according to the spectral responsivities from the absolute calibration. The results show good agreement between the measured and calculated photocurrents within the combined calibration uncertainty at the monochromator-based facility. Furthermore, thermodynamic temperatures of the fixed-point blackbodies with estimated uncertainties ($k = 1$) are also presented in Table 2. Using these experimentally determined thermodynamic temperatures, the $T - T_{90}$ value at the gold point is 52 mK and at the copper point is −50 mK.

5 Discussion and Outlook

In this investigation, an OSRAM 75 W Xe lamp* with a maximum radiance around the bandpass of the radiation thermometers at 650 nm has already been used. With this setup, the signal-to-noise ratio of the LP3 photocurrent for the absolute calibration at the monochromator-based facility is currently limited to 10^3 with a spectral bandwidth of 1 nm. The output radiant power could be further increased by adapting the f-number of the Xe-arc lamp to the used monochromator. Another solution to increase the signal level of the setup could be possible by applying novel radiation sources such as supercontinuum lasers or laser driven lamps as input sources for the monochromator. The continuous spectrum laser sources are currently available with a spectral power of up to 5 mW $\cdot$ nm^{-1}; however, their instabilities due to noise are more than 0.4 % for an average time of 30 s and they are also wavelength dependent [15].

The comparison of the measured thermodynamic temperatures with the ITS-90 temperatures shows $T - T_{90} = 52$ mK for the gold and $T - T_{90} = -50$ mK for the copper freezing-point temperature. In comparison to the current best estimated values of $T - T_{90}$ in Ref. [16], the determined $T - T_{90}$ value at the PTB Au primary fixed

point shows good agreement. With regard to the Cu point, the $T - T_{90}$ value seems to be lower than the best estimate and also well outside its elaborated uncertainty, but well within the obtained measurement uncertainty. One reason for this result is attributed to the impurity of the copper fixed-point material in the blackbody crucible due to its small cell design, for which the original intention was to investigate plateau lengths and not thermodynamic temperature measurements. Therefore, a new Cu cell blackbody will be fabricated and applied in the future to determine the thermodynamic temperature of the Cu point with higher accuracy.

Additionally, the measurements should be performed also with a 950 nm interference filter to evaluate the consistency of the measurement at various wavelengths. However, the absolute calibration for the LP3 at this wavelength region was not possible at that time due to further decreasing radiant power in this wavelength range.

Acknowledgments The authors gratefully acknowledge the help of Elzbieta Kosubek for measuring an effective area of the aperture. Fruitful discussion with E. Schreiber, A. Sperling, and M. Schuster is gratefully acknowledged.

References

1. D.R. Taubert, J. Hartmann, J. Hollandt, J. Fischer, in *Temperature, Its Measurement and Control in Science and Industry*, vol. 7, part 1, ed. by D.C. Ripple (AIP, New York, 2003), pp. 7–12
2. K. Anhalt, J. Hartmann, D. Lowe, G. Machin, M. Sadli, Y. Yamada, Metrologia **43**, S78 (2006)
3. S.W. Brown, G.P. Eppeldauer, K.R. Lykke, Appl. Opt. **45**, 8218 (2006)
4. V.E. Anderson, N.P. Fox, D.H. Nettleton, Appl. Opt. **31**, 536 (1992)
5. Y. Ichino, I. Saito, Y. Yamada, J. Ishii, Spectral Radiance Responsivity Calibration Facility for Thermodynamic Temperature Determination. Presented at TEMPMEKO 2007, 10th International Symposium on Temperature and Thermal Measurements in Industry and Science, Lake Louise, Canada (2007)
6. A. Sperling, O. Larionov, U. Grusemann, S. Winter, in *Proceedings of NEWRAD 2005*, ed. by J. Groebner (PMODWRC, Davos, Switzerland, 2005), p. 93
7. K. Anhalt, A. Zelenjuk, D.R. Taubert, T. Keawprasert, J. Hartmann, Int. J. Thermophys. **30**, 192 (2009)
8. V. Ahtee, S.W. Brown, T.C. Larason, K.R. Lykke, E. Ikonen, M. Noorma, Appl. Opt. **40**, 4228 (2007)
9. H.W. Yoon, C.E. Gibson, V. Khromchenko, G.P. Eppeldauer, R.R. Bousquet, S.W. Brown, K.R. Lykke, Int. J. Thermophys. **29**, 285 (2008)
10. T. Keawprasert, K. Anhalt, R.D. Taubert, A. Abd-Elmageed, A. Sperling, J. Hartmann, in *Proceedings of NEWRAD 2008, 10th International Conference on New Development and Applications in Optical Radiometry*, ed. by Dong-Hoon Lee (KRISS, Daejeon, Korea, 2008), p. 287
11. J. Hartmann, Phys. Rep. **469**, 205 (2009)
12. H.C. McEvoy, The Examination of Base Parameters for ITS-90 Scale Realisation in Radiation Thermometry, *EUROMET.T-S1 Main Measurement Report Final Report* (NPL, United Kingdom, 2007)
13. J. Fischer, H.J. Jung, Metrologia **26**, 245 (1989)
14. K. Anhalt, Y. Wang, Y. Yamada, J. Hartmann, Int. J. Thermophys. **29**, 969 (2008)
15. J.T. Woodward, A.W. Smith, C.A. Jenkins, C. Lin, S.W. Brown, K.R. Lykke, Metrologia **46**, 277 (2009)
16. www.bipm.org/cc/CCT/Allowed/24/D13_rev_WG4_report_CCT_25_June_2008.pdf